



Rapid Mechanical Properties of Multi-layer Film Stacks

Application Note

Jennifer Hay,
Agilent Technologies

Abstract

In this work, we measure the mechanical properties of 50 nm films with remarkable precision and accuracy. The precision is due to Express Test, which performs indentations at a rate of one per second, thereby allowing many indentations to be included in the final determination of modulus and hardness. The accuracy is due, in part, to an analytic model which yields the substrate-independent moduli of thin films. In order to apply the thin-film model to a stack of multiple films, the film modulus of each new layer is determined and then used as the “substrate” modulus for the next layer. This process could be repeated *ad infinitum*. The thin-film model reveals a large difference in Young’s modulus between two 50 nm films.

Agilent’s most recent leap in technology, Express Test, improves our ability to characterize thin films by dramatically increasing the number of independent measurements which can be made in a given time period. Why is it important to make more measurements on thin films? It is important, because nanoindentation measurements of Young’s modulus and hardness tend to grow more scattered as the indentation depth decreases, primarily due to surface roughness, but more scatter can be overcome with more measurements. Express Test is Agilent’s proprietary technology for rapid indentation. Express Test performs indentations in less than five seconds, thus dramatically increasing the number of statistically independent measurements which can be made in a given time period.

Introduction

The primary motivation behind nanoindentation has always been the desire to measure the mechanical properties of small volumes of material, especially in the form of thin films. In the present application, we see how two recent developments in nanoindentation work together to allow the quantitative characterization of films as thin as 50 nm.

For all its advantages, Express Test is nanoindentation at its simplest. The indenter approaches the test surface until contact is detected, loads to achieve the target force or displacement, withdraws the indenter from the sample, and then moves the sample into position for the next indentation. The contact stiffness is calculated using the upper 50% of the unloading curve (i.e. forces which are greater than 50%



Agilent Technologies

of the peak force, and corresponding displacements, acquired during unloading). All downstream calculations such as contact depth, contact area, hardness and Young's modulus are calculated according to established norms, and Young's moduli measured by Express Test agree with values measured by other means for a wide variety of materials. Express Test derives its speed not from novel procedures or analyses, but from a comprehensive understanding of instrument dynamics, combined with strategic advances in data acquisition and storage [1].

Like other indentation methods, Express Test returns a triplet of force, displacement, and stiffness for each indentation, but this information is only as good as the model which relates these fundamental measurements to useful mechanical properties, such as Young's modulus and hardness. The most basic, and oft-cited, model for interpreting fundamental indentation measurements is due to Ian Sneddon, but Sneddon's model presumes that the test material is large and uniform throughout [2, 3]. When applied to thin films, Sneddon's model may return values for Young's moduli that are unduly affected by the

properties of the supporting substrate. However, Agilent's proprietary thin-film model fully accounts for substrate influence, regardless of whether the film is stiffer or more compliant than the substrate. The details of this model are provided elsewhere, and are not reiterated here [4, 5].

In the present application, we show how these two advances, Express Test and thin-film modeling, combine to dramatically improve thin-film characterization. Figure 1 shows a schematic of the unique material tested in this work. The substrate is a sintered composite of alumina (Al_2O_3) and titanium carbide (TiC), the microstructure of which is shown in Figure 2. Upon this substrate is a layer of sputter-deposited Al_2O_3 having a thickness of 2600 nm. The topmost layer of this structure is 50 nm of either silica (SiO_2) or alumina (Al_2O_3). The properties of each layer are not only important in their own right, but also must be known in order to accurately calculate the properties of subsequent layers via the thin-film model. Thus, in this work, we provide a practical procedure for determining the properties of individual layers in a multi-layer stack.

Experimental Method

Samples

The samples identified in Table 1 were tested. Basically, the substrate was tested alone (sample 1) and then subsequent layers were tested as they were deposited.

Equipment and Procedure

All samples were tested with an Agilent G200 NanoIndenter, configured with the Express Test option. All tests were performed using a DCM II head fitted with a Berkovich indenter. Sample positioning was accomplished with the NanoVision option. This combination of hardware (the DCM II and NanoVision stage) allowed Express Test to perform one indentation every second.

Preliminary testing was done on sample 2 in order to know the depth profile of properties for this material. This preliminary test was accomplished with the method "Express Test, Varied Force" which automatically performs an array of 20×20 indentations over an appropriate range of forces within a $100 \mu m \times 100 \mu m$ domain.

For final testing, 16 indentation arrays were performed on each of the four

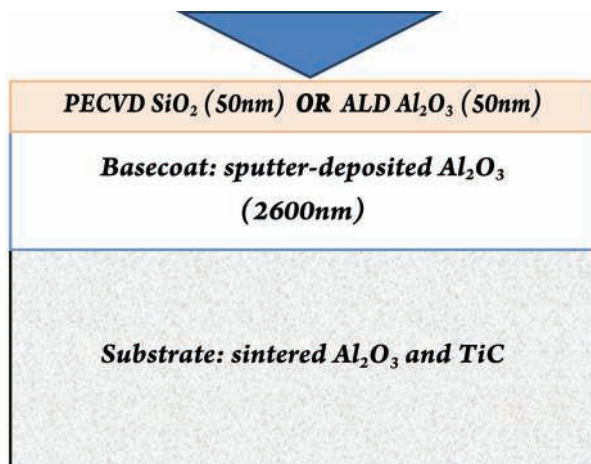


Figure 1. Schematic of film stack (not to scale).

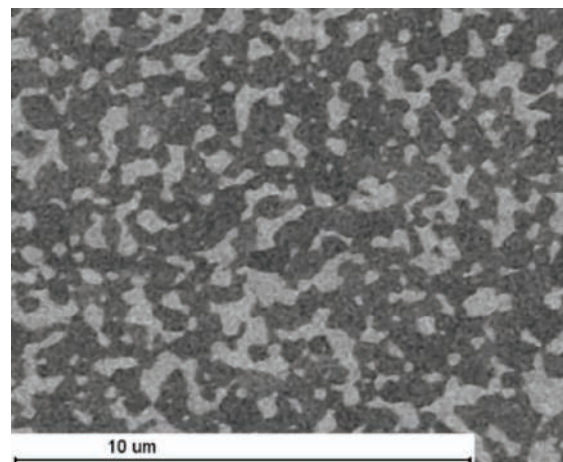


Figure 2. Scanning-electron micrograph of bare substrate. TiC grains are light and Al_2O_3 grains are dark.

Sample ID	Description	Film Thickness, nm	Indentation Depth, nm	Hardness, GPa	Apparent Modulus, GPa	Film Modulus, GPa
1	Substrate: Sintered composite of alumina, Al ₂ O ₃ , and titanium carbide, TiC (Fig. 1)	N/A	89.8	28.5±0.61	471.5±7.3	N/A
2	Basecoat: Alumina, sputter-deposited on substrate (SD Al ₂ O ₃)	2600	158.7	8.95±0.02	159.5±0.5	146.4±0.5
3	Silica applied to basecoat by plasma-enhanced chemical-vapor-deposition (PE CVD SiO ₂)	50	21.7	6.55±0.12	99.0±1.8	56.3±1.0
4	Alumina applied to basecoat by atomic-layer deposition (ALD Al ₂ O ₃)	50	22.8	8.07±0.13	143.7±2.5	134.9±2.3

Table 1. Properties of each layer in the multi-layer stack depicted schematically in Figure 1. Testing time for each sample (16 arrays of 25 indents) was just under an hour.

samples. Each indentation array comprised 25 indentations within a domain of 100 μm x 100 μm. Thus, a total of 400 indentations were performed on each sample: 16 arrays x 25 indents per array = 400 indents. The sixteen arrays were systematically arranged so as to cover a total area of about 1 cm². For each array of 25 indents, the median values of Young's modulus and hardness were calculated. Reported properties and uncertainties are the average and standard deviation, respectively, of these 16 medians.

The peak indentation force or displacement was set with consideration for the scale of the material. For samples 1 and 2, the substrate alone and with a basecoat, all indentations were performed with the method "Express Test to a Force, Batch" using a peak force of 5mN. For samples 3 and 4, all indentations were performed with the method "Express Test to a Displacement, Batch" using a peak displacement of 20 nm (40% of the film thickness).

Thin-film Analysis for Young's Modulus

The true "film" moduli of progressive layers were calculated by considering the influence of supporting layers. For sample 1, which was the substrate alone, the calculation of Young's modulus was straightforward, because the material volume was large (relative to the indentation size) and properties were uniform. Thus, the Young's modulus of sample 1, which we shall call E_1 , was calculated according to Sneddon's analysis as developed by Oliver and Pharr for instrumented indentation [3]. For sample 2, which comprised a basecoat applied to the substrate, Young's modulus was calculated in two ways. First, the "apparent" modulus, which we shall call E_2 , was calculated in the same way as E_1 , that is, according to Sneddon's analysis as developed by Oliver and Pharr. But in addition, we also calculated a "film" modulus for sample 2, E_{f2} , via Agilent's thin-film model which requires prior knowledge of the substrate modulus, E_1 , the apparent modulus, E_2 , the indentation depth, h_2 , and the film thickness t_2 [5]. Thus, without delving

into the details, we may state simply that the true "film" modulus of the second sample was calculated as:

$$E_{f2} = f(E_1, E_2, h_2, t_2).$$

The moduli of the topmost films, samples 3 and 4, were calculated analogously. First, "apparent" moduli, E_3 and E_4 , were calculated according to Sneddon's analysis as developed by Oliver and Pharr. Then, "film" moduli were calculated via Agilent's thin-film model by considering the basecoat as the "substrate," and its modulus, E_{f2} , as the "substrate" modulus. That is, we calculated

$$E_{f3} = f(E_{f2}, E_3, h_3, t_3), \text{ and}$$

$$E_{f4} = f(E_{f2}, E_4, h_4, t_4).$$

In summary, the true film modulus of each new layer is calculated using the true modulus of the previous layer as the "substrate" modulus. Although this multi-stack only comprised a substrate and two films, the analytic process described here could be repeated *ad infinitum*.

Results and Discussions

Table 1 summarizes the Young's modulus and hardness for each of the four samples tested in this work. Let us examine these results in more detail.

The modulus and hardness for the composite substrate, $E_1 = 471.5 \pm 7.3$ GPa and $H_1 = 28.5 \pm 0.61$ GPa, are comparable to what others have measured for bulk Al_2O_3 and TiC. For example, in their inaugural paper on nanoindentation, Oliver and Pharr measured the modulus and hardness of single-crystal Al_2O_3 to be 441 GPa and 30 GPa, respectively. For the ceramic form of titanium carbide at room temperature, the CRC Handbook gives the modulus as 439 GPa and a Vickers hardness of 2900–3200 kg/mm² [6], which translates to a nanoindentation hardness of 30–34 GPa [7]. Sintering these two materials together in a fine-grained form does not appear to substantially compromise the mechanical properties of the resulting composite.

Yet, one may wonder whether the large number of indentations afforded by Express Test might reveal slight differences between the component materials. The indentation depth, 90 nm, is less than 10% of the diameter of a typical grain, which is about 1 μm (Figure 2). Thus, we should expect many indentations to probe single grains. The histograms in Figure 3, which include results from all 400 indentations on the substrate, assure us that even at this scale, the two materials are indistinguishable. These histograms are nearly Gaussian and do not manifest independent peaks for the two components. Thus, we conclude that the component materials are mechanically so similar that even 400 indentations cannot distinguish them.

The modulus and hardness of the sputter-deposited Al_2O_3 basecoat, $E_{f2} = 146.4 \pm 0.5$ GPa, and $H_2 = 8.95 \pm 0.02$ GPa, are much lower than the properties

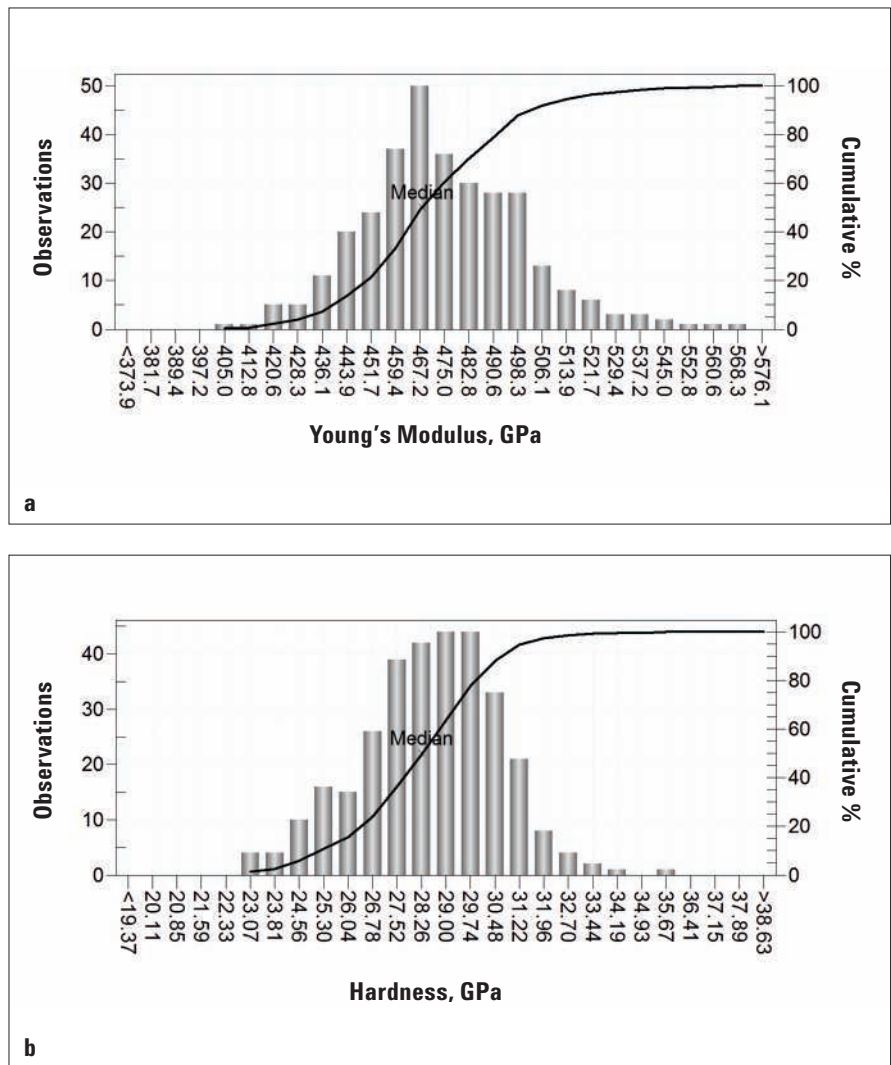


Figure 3. Histograms of 400 indentations on substrate. Al_2O_3 and TiC grains are not distinguishable. Histograms are automatically generated in NanoSuite.

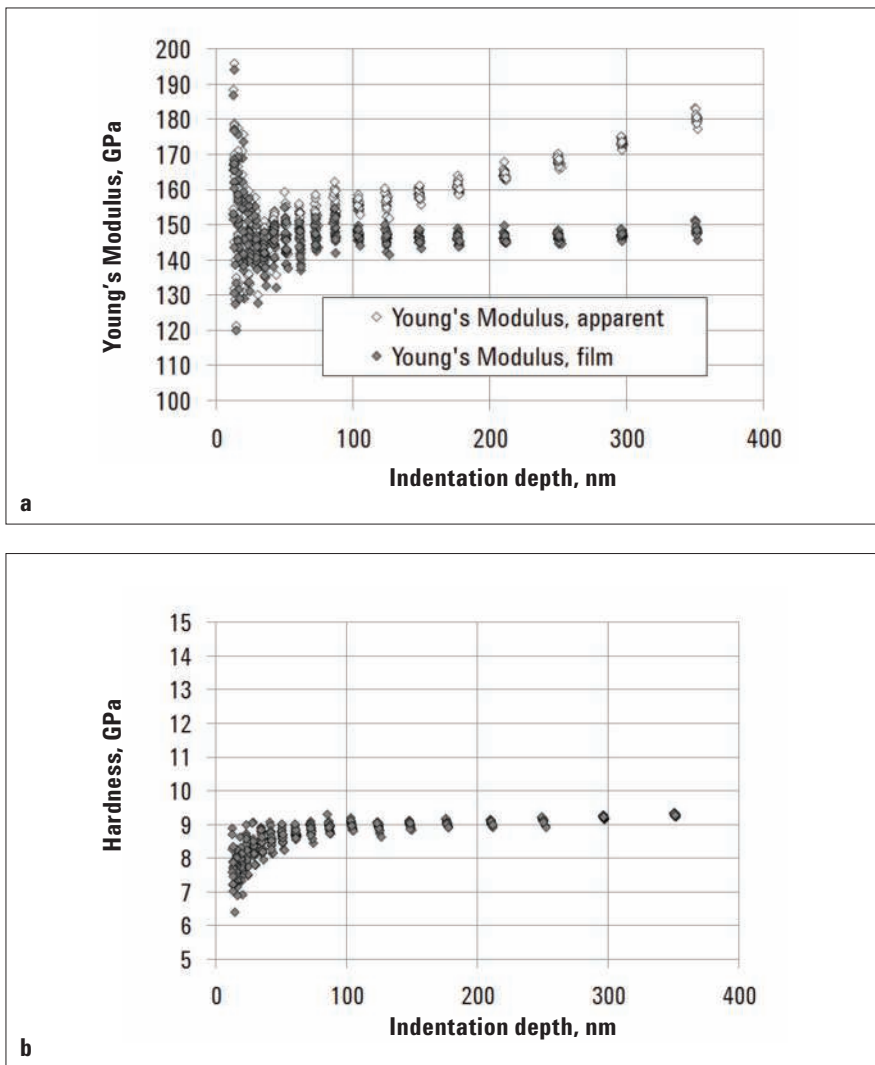


Figure 4. Depth profiles of (a) modulus and (b) hardness for sample 2, sputter-deposited Al_2O_3 ($t_2 = 2600\text{nm}$) on substrate. Testing time was 10 minutes. Apparent modulus manifests increasing influence of substrate with indentation depth, but film modulus is constant. Hardness increases until the indentation is deep enough to be fully plastic, then remains constant for larger depths.

of single-crystal alumina. However, the point-to-point consistency is remarkable; the standard deviation among the 16 median observations is less than 0.4% of the average! The apparent modulus, $E_2 = 159.5 \pm 0.5$ GPa, is only slightly elevated due to substrate influence, because the indentation depth ($h_2 \approx 160\text{nm}$) is only 6% of the film thickness ($t_2 = 2600\text{nm}$). Although the elevation of E_2 is slight, it is significant. The common rule is that substrate influence need not be accounted, so long as the indentation depth is less than 10% of the film thickness. However the fact that E_2 is 9% greater than E_{f2} demonstrates that substrate influence may be significant even when the indentation depth is less than 10% of the film thickness. Figure 4 shows the results of the preliminary testing on this sample, which was done to establish the depth profile in properties. Figure 4a reveals that for larger indentation depths, the apparent modulus (light symbols) increases due to the increasing influence of the substrate. However, when the thin-film model is applied, the substrate influence is removed, and the film modulus (dark symbols) is independent of indentation depth, as it should be. Interestingly, the hardness plotted in Figure 4b manifests little substrate influence, even when the indentation depth is 10% of the film thickness. Unlike modulus, there is no need for a corrective model for hardness, because the zone of plastic deformation, the resistance to which is quantified by the hardness, is much smaller than the zone of elastic deformation. The slight increase in hardness observed at depths greater than 300 nm is likely due to the onset of substrate influence.

There is one more feature to note about Figure 4b. As the indentation depth approaches zero, the hardness decreases. This is not due to any deficiency or change in the film in

this region, but rather due to the elastic nature of such small contacts. In order to measure a meaningful value of hardness, one must cause plasticity in the test material. However, due to the hardness of the film, and finite rounding at the apex of the diamond indenter, indents which are smaller than about 90 nm are increasingly elastic, resulting in a lower value of hardness. In fact, Figure 4 guided the choice of a test force for final testing on sample 2. Being in possession of the preliminary data plotted in Figure 4, we chose an indentation force of 5 mN for final testing, because the resulting indentation depth, about 160 nm, was large enough to be fully plastic, but not so large as to be unduly influenced by the substrate. Presently, we note that at 20 nm, the measured hardness of sample 2 is only 7.8 ± 0.4 GPa¹, and we shall refer back to this fact when we discuss the results for sample 4, which were obtained at the same depth.

When comparing samples 3 and 4, the first thing to note is the outstanding precision. With an indentation depth of only about 20 nm, the standard deviation is less than 2% of the value. This precision is due to Express Test, because 25 indents (one array) go into the determination of a median, and this process is repeated 16 times across the sample surface. Thus, the standard deviation among the 16 medians is extraordinarily small. As expected, more measurements increase precision.

The alumina film (sample 4) has significantly higher modulus and hardness than the silica film (sample 3). Figure 5 compares the moduli of the two films. Because the indentation depth is 40% of the film thickness, the substrate influence on the apparent modulus is substantial. Without the thin-film model, the moduli seem rather similar: $E_3 = 99$ GPa vs. $E_4 = 144$ GPa. But in actuality, the discrepancy in moduli is much greater. With the substrate influence accounted and removed, we

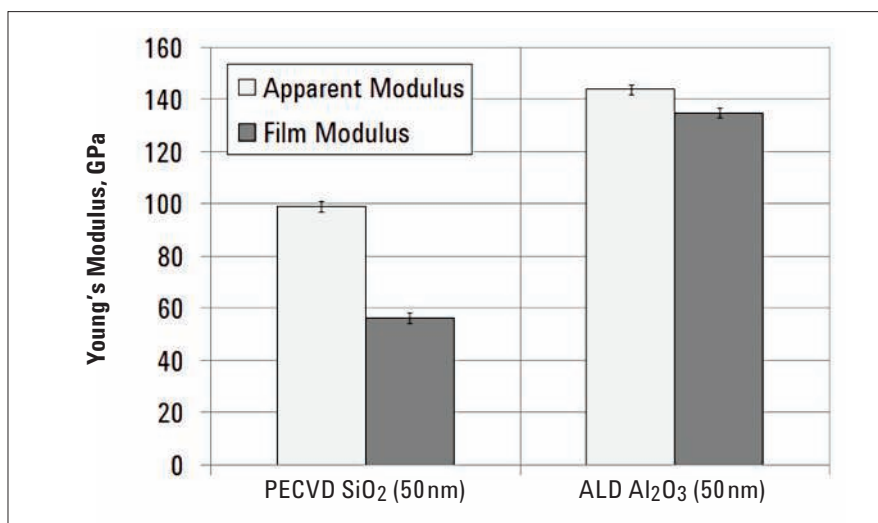


Figure 5. Moduli of topmost films, both with (dark) and without (light) correction for substrate influence. Silica film manifests more substrate influence due to greater difference between film and substrate properties. True difference between SiO₂ and Al₂O₃ films is only evident when moduli are corrected with Agilent's elastic thin-film model.

find that $E_{f3} = 56$ GPa vs. $E_{f4} = 135$ GPa. Drawing conclusions from the direct moduli alone might lead to poor engineering decisions about which material to use in production.

Although the measured hardness of sample 4 ($H_4 = 8.07 \pm 0.13$ GPa) is less than that of sample 2 ($H_2 = 8.95 \pm 0.02$ GPa) it would be a mistake to conclude that atomic-layer deposition is inferior to sputter deposition. The hardness of sample 2 was measured at a depth of about 160 nm, under fully plastic conditions. Due to the thinness of the film, the hardness of sample 4 was measured at only 20 nm where we don't expect full plasticity. In fact, these measurements lead to the provisional conclusion that atomic-layer deposition is superior, because the measured hardness ($H_4 = 8.07 \pm 0.13$) is greater than that measured at a similar depth on the sputter-deposited alumina (7.8 ± 0.4 GPa¹). To increase our confidence in this conclusion, the two films would need to be deposited to the same thickness, preferably more than 200 nm, and tested with identical methods.

Conclusions

The substrate, a sintered composite of alumina (Al₂O₃) and titanium carbide (TiC), has properties which are remarkably similar to bulk versions of the component materials. Even for indentations which are substantially smaller than the grain diameter, no difference between Al₂O₃ and TiC grains is discerned. As expected, the 50 nm layer of atomic-layer deposited alumina (ALD Al₂O₃) is harder and has a higher modulus than the 50 nm layer of plasma-enhanced, chemical-vapor deposited silica (PE CVD SiO₂), although to some extent, the difference is masked by substrate influence. When substrate influence is removed via the thin-film model, the difference between the two films is much clearer. With an indentation depth of only 20 nm, the hardness measurements on the ALD Al₂O₃ and PE CVD SiO₂ are somewhat compromised by elasticity. Nevertheless, we confirm that atomic-layer deposition is superior to sputter deposition.

¹ Unlike the results in Table 1, this value represents the average and standard deviation of properties from only 20 indents along a 100 μm-vector.

References

1. Hay, J. and Horwitz, J., "Revolutionary Agilent Express Test Option for the Nano Indenter G200," Agilent Technologies, 2012, Document No: 5990-9948EN Rev. C, Date Accessed: January 27, 2014; Available from: <http://cp.literature.agilent.com/litweb/pdf/5990-9948EN.pdf>.
2. Sneddon, I.N., "The Relation Between Load and Penetration in the Axisymmetric Boussinesq Problem for a Punch of Arbitrary Profile," *Int. J. Eng. Sci.* 3(1), 47–57, 1965.
3. Oliver, W.C. and Pharr, G.M., "An Improved Technique for Determining Hardness and Elastic-Modulus Using Load and Displacement Sensing Indentation Experiments," *Journal of Materials Research* 7(6), 1564–1583, 1992.
4. Hay, J.L. and Crawford, B., "Measuring Substrate-Independent Modulus of Thin Films," *Journal of Materials Research* 26(6), 2011.
5. Hay, J.L., "Measuring Substrate-Independent Young's Modulus," Agilent Technologies, Inc., 2010, Document No: 5990-6507 EN, Date Accessed: August 31, 2010; Available from: <http://cp.literature.agilent.com/litweb/pdf/5990-6507EN.pdf>.
6. Shackelford, J.F., Alexander, W., and Park, J.S., eds., *CRC Materials Science and Engineering Handbook*, 2nd ed. Boca Raton: CRC Press, 1994, pp. 471, 508.
7. Hay, J., "The Revolutionary Impact of the Oliver and Pharr Technique on the Science of Hardness Testing," Agilent Technologies, 2013, Document No: 5991-3250EN, Date Accessed: January 28, 2014; Available from: <http://cp.literature.agilent.com/litweb/pdf/5991-3250EN.pdf>.

Nanomeasurement Systems from Agilent Technologies

Agilent Technologies, the premier measurement company, offers high-precision, modular nanomeasurement solutions for research, industry, and education. Exceptional worldwide support is provided by experienced application scientists and technical service personnel. Agilent's leading-edge R&D laboratories ensure the continued, timely introduction and optimization of innovative, easy-to-use nanomeasure system technologies.

www.agilent.com/find/nano

Americas

Canada	(877) 894 4414
Latin America	305 269 7500
United States	(800) 829 4444

Asia Pacific

Australia	1 800 629 485
China	800 810 0189
Hong Kong	800 938 693
India	1 800 112 929
Japan	0120 (421) 345
Korea	080 769 0800
Malaysia	1 800 888 848
Singapore	1 800 375 8100
Taiwan	0800 047 866
Thailand	1 800 226 008

Europe & Middle East

Austria	43 (0) 1 360 277 1571
Belgium	32 (0) 2 404 93 40
Denmark	45 70 13 15 15
Finland	358 (0) 10 855 2100
France	0825 010 700*
	*0.125 €/minute
Germany	49 (0) 7031 464 6333
Ireland	1890 924 204
Israel	972-3-9288-504/544
Italy	39 02 92 60 8484
Netherlands	31 (0) 20 547 2111
Spain	34 (91) 631 3300
Sweden	0200-88 22 55
Switzerland	0800 80 53 53
United Kingdom	44 (0) 118 9276201

Other European Countries:

www.agilent.com/find/contactus

Product specifications and descriptions in this document subject to change without notice.

© Agilent Technologies, Inc. 2014
Published in USA, February 17, 2014
5991-4077EN



Agilent Technologies